The evolutionary thermal performance and development of a novel thermal diode pre-heat solar water heater under simulated heat flux conditions

*M Smyth, P. Quinlan, JD Mondol, A. Zacharopoulos, D McLarnon and A Pugsley

*Centre for Sustainable Technologies, School of the Built Environment,

Ulster University, Newtownabbey BT37 0QB, N. Ireland.

Tel: ++44(0)2890368119, Fax: ++44(0)2890368239, e-mail: m.smyth1@ulster.ac.uk

ABSTRACT

This paper presents the development through experimental performance characterisation of a pre-heat ICSSWH that utilises a novel thermal diode operation to reduce ambient heat loss during non-collection periods. Using a bespoke thermal flux simulation test facility, 4 prototype versions of the pre-heat thermal diode ICSSWH were produced and evaluated (Mark I to IV) at Ulster University. Each prototype was developed and evolved on the previous design, encompassing performance improvements and fabrication enhancements. The concept has been designed and developed to be a sustainable, pre-heat alternative to other solar water heating systems traditionally used in DHW installations in retro-fit and social housing applications. The highest 6 hour and 3 hour collection efficiency was 33.2% and 41.97%, respectively under thermally simulated conditions for a unit with capillary matting and 150mbar internal pressure (MIIIb 17). The lowest system 'U' value was 0.98 W $m^{-2}K^{-1}$ (long and thin raised pockets, MIV 12) under thermal (solar) flux simulation testing and no draw-off conditions. When the current prototype ICS units are compared with other conventional ICS systems, particularly in terms of thermal retention during non-collection periods, an improved performance is clearly demonstrated. The measured thermal losses were approximately 50% less than other similarly measured systems.

Keywords

ICSSWH, pre-heat, thermal flux simulation, thermal diode

1.1 Introduction

Integrated Collector Storage Solar Water Heaters (ICSSWH) are simple, low cost solar devices. The development of these systems is detailed in Smyth et al [1]. They suffer however significant ambient heat loss, especially at night-time and during non-collection periods [2].

Several studies have been carried out focusing on the improvement of the thermal performance of ICSSWH systems, primarily during night operation. Previous ICSSWH designs have attempted to improve thermal energy storage during non-collection periods by; (i) reducing heat loss from the aperture [3][4][5][6], (ii) reducing convective heat transfer in the collector cavity from the store to the aperture [2] or (iii) reducing heat transfer from the store surface [7][8][9]. Studies to reduce night-time thermal losses include the use of two stores [10]. The use of low pressure and Phase Change Materials (PCM), such as water, within an ICS unit was first suggested by De Beijer [11]. The evaporator is the collector absorbing surface and the condenser is the surface of the inner storage vessel. The working principle exploits the latent heat transfer characteristics of liquid to gas

phase change whilst reducing heat loss during non-collection periods. The work presented in this paper details the experimental characterisation of a pre-heat ICSSWH that utilises the novel thermal diode operation presented by De Beijer [11].

1.2 Description of the pre-heat thermal diode ICSSWH

The conceptual pre-heat thermal diode ICSSWH is constructed from 3 concentric tubes. The outer tube forms the aperture and unit casing. It is made from a transparent material such as glass or Perspex. Its role is to protect the absorbing surface of the next vessel and reduce convective heat loss as well as defining the initial physical appearance of the unit, as shown in Figure 1. The remaining tubes (vessels) combine to create the collector/storage element and are arranged to create an annular space between the concentric walls of these inner and outer vessels.

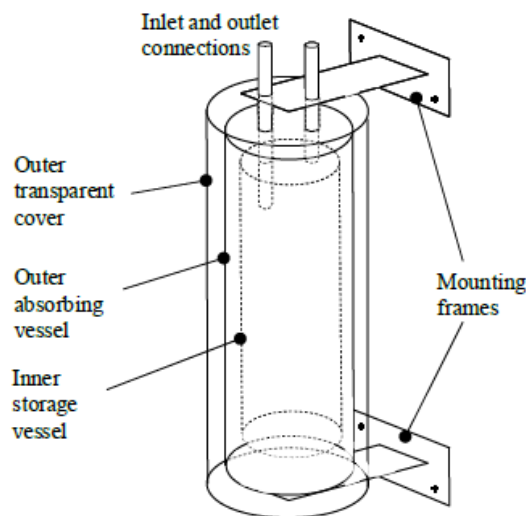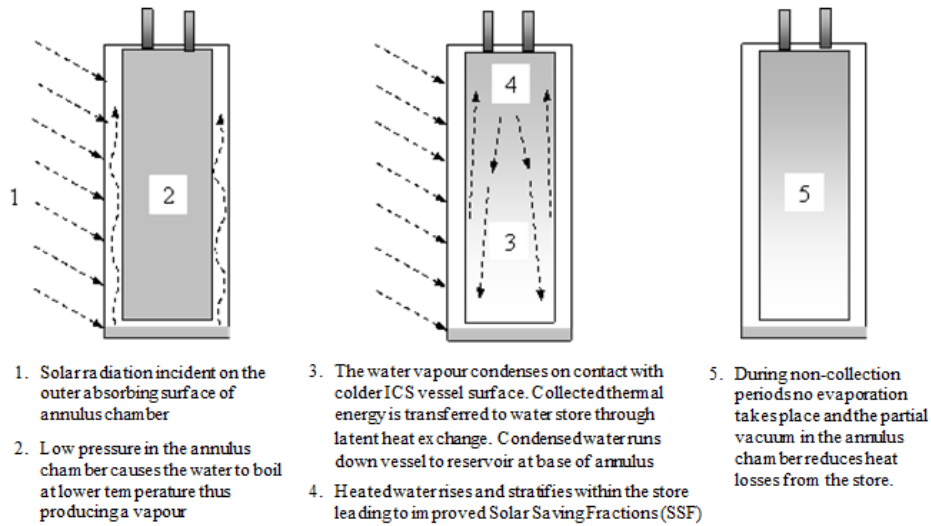Figure 1: The initial conceptual design of the pre-heat thermal diode ICSSWH

The annular space is partially evacuated to a near vacuum condition and contains a small amount of a liquid/vapour PCM (phase change material). Just like a thermal diode, the design promotes solar collection but reduces thermal losses. During collection periods, solar radiation incident on the outer absorbing surface of annulus chamber (coated with a selective film) causes the PCM in contact with the surface to evaporate at low temperature thus producing a vapour. The PCM vapour condenses on contact with colder inner vessel surface and the collected thermal energy is transferred to water store through latent heat exchange. Condensed PCM runs down the vessel to a reservoir at base of annulus to continue the cycle. During non-collection periods no evaporation takes place due to the partial vacuum in the annulus chamber, thereby reducing heat loss from the store. The generic system operation is illustrated in Figure 2. The annular space can be partially filled with a liquid/vapour phase change material. Water is the most cost effective and environmentally benign PCM, although many other materials may be employed such as alcohols and commercial refrigerants.

1. Solar radiation incident on the outer absorbing surface of annulus chamber

2. Low pressure in the annulus chamber causes the water to boil at lower temperature thus producing a vapour

3. The water vapour condenses on contact with colder ICS vessel surface. Collected thermal energy is transferred to water store through latent heat exchange. Condensed water runs down vessel to reservoir at base of annulus

4. Heated water rises and stratifies within the store leading to improved Solar Saving Fractions (SSF)

5. During non-collection periods no evaporation takes place and the partial vacuum in the annulus chamber reduces heat losses from the store.

Figure 2: Schematic detail of operation principle of the pre-heat thermal diode ICSSWH

A total of 4 prototype versions of the pre-heat thermal diode ICSSWH were produced and evaluated (Mark I to IV). Each prototype developed and evolved on the previous design, encompassing performance improvements and fabrication enhancements as detailed in Table 1 and Figure 3. Where possible the units were fabricated and assembled at Ulster University, with one-off components out-sourced from local fabrication specialists. The units presented for comparison in this particular study comprise of a basic control unit and a series of optimised units using enhanced heat transfer elements.

Table 1: Variants Mark I-IV and enhancements

| Variant	Description	Mass (kg)	Thermal mass (kJ/K)	Outer vessel surface area (m^2)	Inner vessel volume (litres)
Mark I	Basic two concentric cylinders design	23.29	10.9	1.08	28.2
Mark II	Mark I with sloped pocket and cowl design	24.03	11.3	1.08	28.2
Mark IIIa/b	Mark I/II with non-conducting connection and top hat divider	25.04	12.5	1.08	28.2
Mark IV	Mark III with elongated pocket and cowl design	24.16	11.3	1.08	28.2
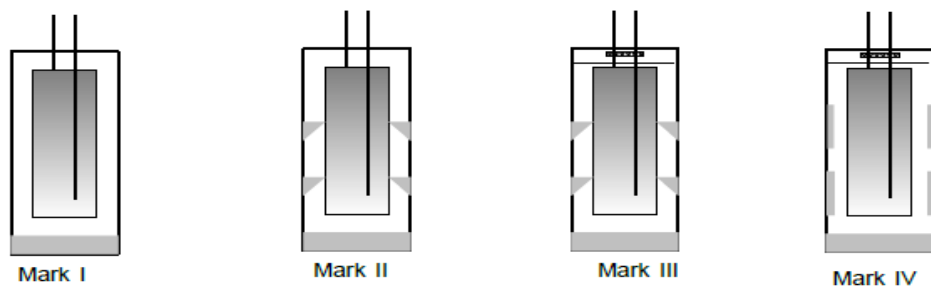
Figure 3: Schematic detail of variants Mark I to IV and enhancements

3

99   The control unit (Mark I) consisted of two vessels, the outer vessel was 300mm Ø (1m in length) and the inner

100   vessel was 200mm Ø (0.9m in length). Both vessels were fabricated from 1.5mm thick stainless steel sheet. Each

101   vessel had a welded base with a flanging arrangement to allow for access and entry for monitoring

102   instrumentation. The other units were based the same dimensional and construction features used in the

103   fabrication of the control unit, but incorporated a number of design enhancements to aid the heat transfer process

104   during the collection phase and reduce heat loss during non-collection periods.

105

106   **1.3 Description of the experimental facility**

107   The experimental performance of the pre-heat thermal diode ICSSWH units was determined using a thermal flux

108   simulation facility at Ulster University. A total of 59 separate experimental procedures were conducted and

109   included the various versions with performance enhancements such as non-conducting inlet and outlet ports,

110   suppression baffles and mechanisms to increase the wetted heat transfer surfaces through a patented cascade

111   design in the annular cavity. Testing was conducted under thermal flux simulation to have a uniform (constant

112   heat input) basis in order to ascertain performance comparison of the various designs.

113

114   The thermal 'solar' simulator comprised of a pair of heater mats positioned unto the outer absorbing surface of

115   the vessel to simulate incident solar flux. T-type copper-constantan thermocouples, which had an error of ± 0.5°C

116   between 0 and 70°C, were used to measure the water storage temperatures within the unit versions, various

117   surface temperatures and ambient air temperature. Temperature, pressure and heat input were recorded through a

118   Delta T logging device linked to a PC, as shown in Figure 4.
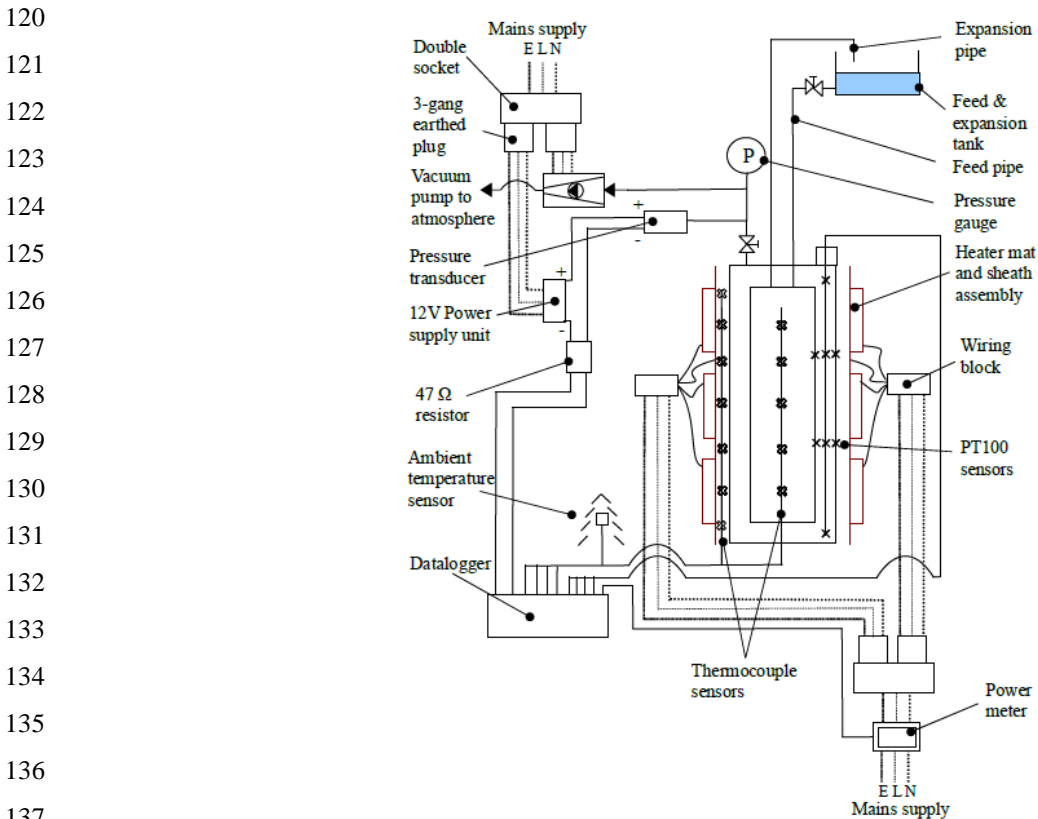
119

Figure 4: Schematic diagram of thermal flux simulation facility

140 **1.4 Description of the experimental procedure**

141 Evaluation of collection and thermal retention performance characteristics were performed using thermal

142 simulation and solar simulation conditions. System performance characterisation was based on BS ISO 9459-

143 5:2007 [12]. No thermal storage draw offs were performed during the tests.

144

145 Under thermally simulated heat flux conditions (heater mats and distribution sheath) combined collection and

146 thermal retention experiments were conducted for Marks I to IV. The tests were conducted over 6 to 24 hours in

147 order to determine the daily collection efficiency (6 hours exposure to thermally simulated (constant) conditions)

148 and thermal retention (18 hours cool down). A period of 6 hours collection was chosen since it compares with the

149 average annual daily utilisable insolation period for the London area (Bracknell) with a total monthly mean daily

150 irradiation on a vertical plane of 2.24 kWh/m^2 [13]. At the beginning of each experiment period the inner vessel

151 was re-filled and the test started with steady ambient temperatures and uniform tank temperatures.

152

153

154

155

156

157

158

159

160

161

162

163

164

165

166 Figure 5: Images of the Mark IV unit under heat flux simulator test conditions

167

168 Figure 5 shows the prototype Mark IV rig prior to insulation, ready for testing. The collection period started

169 when the heater mats were turned on and the assembly monitored for six hours after which the heater mats were

170 turned off. The insulation around the unit was removed after the collection period and the cool down period

171 started. After a further 18 hour period the experiment was complete. Test information from the data logger was

172 then downloaded for analysis.

173

174 **1.5 Experimental results and analysis**

175 The experimental performance of each unit was determined from the experimental data retrieved from the

176 extensive testing programme. Thermal store, annulus and external environment were analysed during testing to

177 determine the system characteristics. Thermal store characterisation used the average normalised temperatures

178 and stratification within the store both on collection and cool down to allow analysis of collection and thermal

179 retention efficiencies and develop hypothesis for heat transfer mechanisms into and within the thermal store.

180 Annulus characterisation used the temperature and partial vacuum pressure measurements during collection and

181 cool down periods to present the temperature distribution and allow analysis of the sensible and latent heat
182 transfer mechanisms taking place. The external environment is not characterised independently but as part of the
183 characterisations within the thermal store and annulus. Experimentally observed temperatures were used to
184 calculate mean temperatures in the thermal store volume (T_{av}). During collection periods, temperatures recorded
185 within the thermal store at the beginning and end of collection were used to calculate average start temperature
186 ($T_{initial}$) and average end temperature (T_{end}). Thermal energy collected (Q_{col}) by the unit was determined by

187

188
$$Q_{col} = mc_p \left(T_{end} - T_{initial} \right) \quad \{1\}$$

189

190 where m is the mass of water in the thermal store and c_p is the specific heat capacity of the water. The unit
191 collection efficiency was determined by

192

193
$$\eta_{col} = \left(\frac{Q_{col}}{Q_{supplied}} \right) \times 100 \quad \{2\}$$

194

195 where $Q_{supplied}$ is the energy supplied over the collection period. The collection efficiency varies depending on the
196 collection time period used therefore during evaluation it was measured over a 6 hour period unless otherwise
197 specified. Thermal stratification within the store is characterised by a stratification index (σ) calculated using
198 equation (3) below [14]

199

200
$$\sigma = \frac{\left(T_{av,t} - T_{av,b} \right)}{\left(T_{av,t} - T_{av,b} \right)_{start}} \quad \{3\}$$

201

202 where $T_{av,t}$ and $T_{av,b}$ are the average thermal store temperatures within the top 1/5 and bottom 1/5 storage volumes
203 and ($T_{av,t} - T_{av,b}$)$_{start}$ is the temperature difference between the top 1/5 and bottom 1/5 storage volumes at the
204 beginning of the collection period. A de-stratification time constant measured as the time it takes for the
205 stratification index σ, to decrease to 0.3679 of its initial value, is used to measure de-stratification during the cool
206 down period. Thermal retention efficiency (η_{ret}) is determined by

207

208

209
$$\eta_{ret} = \left(\frac{m \times c_p \left(T_{final} - T_{amb} \right)}{m \times c_p \left(T_{initial,c} - T_{amb} \right)} \right) \times 100 \quad \{4\}$$

210

211 where $T_{initial,c}$ is the average temperature at the start of the cool-down period, T_{final} is the average temperature at
212 the end of the cooling period and T_{amb} is the average ambient temperature throughout the cool-down period.

213

214 The system heat loss coefficient also known as the system 'U' value was calculated from equation (5) [15]

215

$$216 \qquad U_{system} = \frac{mc_{system}}{A_{unit}\Delta t} \ln\left(\frac{\left(T_{initial,c} - T_{amb}\right)}{\left(T_{final} - T_{amb}\right)}\right) \qquad \{5\}$$

217

218   where mc$_{system}$ is the thermal mass of the system based on the mass and specific heat capacity of the individual

219   units and A$_{unit}$ is the surface area of the outer vessel.

220

1.6 Discussion

222   The Mark I unit was the first prototype tested. Four collection and cool-down tests were undertaken. With test MI

223   1 the control with no PCM at atmospheric pressure (1013mbar) and MI 4 with 3 litres of PCM at 50mbar and

224   with capillary matting. Figure 6 shows the normalised average water temperatures within the thermal store over

225   the collection and cool down for each test. Mark I 1 had a base collection efficiency of 21.57% whilst the

226   improved (evacuated) Mark I 4 had a collection efficiency of 25.39%. The 18 hour heat retention efficiencies and

227   system heat transfer coefficients for Mark I tests 1 to 4 and 24 hour heat retention efficiencies and system heat

228   transfer coefficients for Mark I tests 5 (1013 mbar) & 6 (100 mbar) are shown in Figure 7.
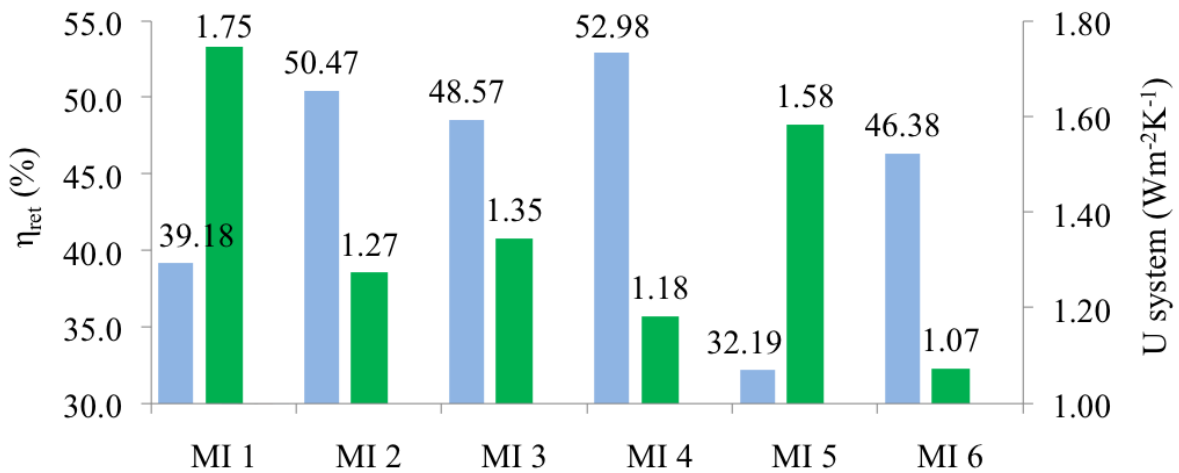
229
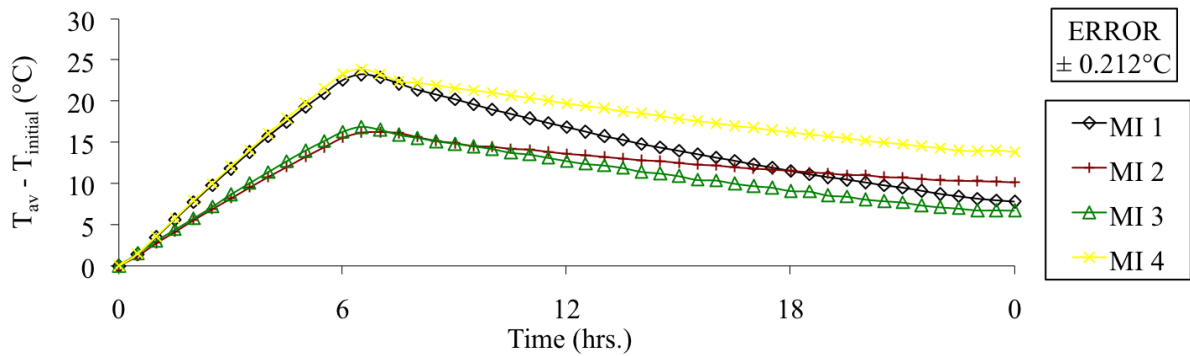
230

231   Figure 6: Normalised average thermal store temperatures for Mark 1 tests 1 to 4 for a 6 hour collection period

232   and 18 hour cooling period under thermally simulated test conditions

233

234

235

236   Figure 7: The 18 hour heat transfer coefficient and retention efficiency during Mark I tests 1 to 4 under cool-

237   down test conditions and tests 5 to 6 under thermal retention test conditions

238

7

239   The highest normalised average thermal store temperatures and the highest collection efficiencies were achieved
240   by MI 4. The collection efficiency was significantly improved by introducing the low pressure environment,
241   PCM and capillary matting. This increase occurred because of lower resistance to heat transfer within the
242   annulus. Stratification of water within the thermal store is important in achieving a high solar savings fraction
243   during partial load draw-offs. During collection the greatest stratification occurred during MI 1 whilst MI 4 was
244   more uniform, indicating that most heat was being transferred at a lower level. MI 1 exhibited the lowest heat
245   retention efficiency and highest system 'U' value whilst MI 4 had the highest heat retention efficiency and lowest
246   system 'U' value as illustrated in Figure 7. Compared to MI 1, MI 4 increased heat retention efficiency by 35%
247   (52.98%) and reduced the system 'U' value by 32.5% (1.18 W $m^{-2}K^{-1}$). The results show that the heat retention
248   efficiency and heat transfer coefficient are proportional to the partial vacuum pressure that was maintained over
249   the cool-down period. More details pertaining to the cool-down period are presented by Quinlan [16].

251   Mark II increased the effective heated surface area in contact with the PCM through the inclusion of raised PCM
252   pockets within the annulus. To prevent the condensate condensing on the inner vessel from flowing back to the
253   bottom of the outer vessel, sloping cowls were paired against the pockets directly opposite on the inner vessel.

255   The normalised average water temperatures for MII 1 to 3 are shown in Figure 8 and corresponding collection
256   efficiencies improved from 25.81% (MII 1) to 29.82% for Mark II 3. The use of the raised pockets and cowl
257   arrangement with capillary matting produced increased collection efficiency, 17.4% more than MI 4. The average
258   normalised store temperature for MII 3, after 6 hours was 45°C, 21°C higher than MI 4. The use of the raised
259   pocket and cowl arrangement also increased stratification (over Mark I) within the thermal store. During the 18
260   hour cool down period, the MII 3 system 'U' value (1.75 W $m^{-2}K^{-1}$) was 32.5% worse than MI 4 (1.18 W $m^{-2}K^{-1}$)
261   and a reduced retention efficiency of 39.24% because of the higher pressure due to higher annulus temperatures
262   and water vapour mass increasing conduction and convection losses.
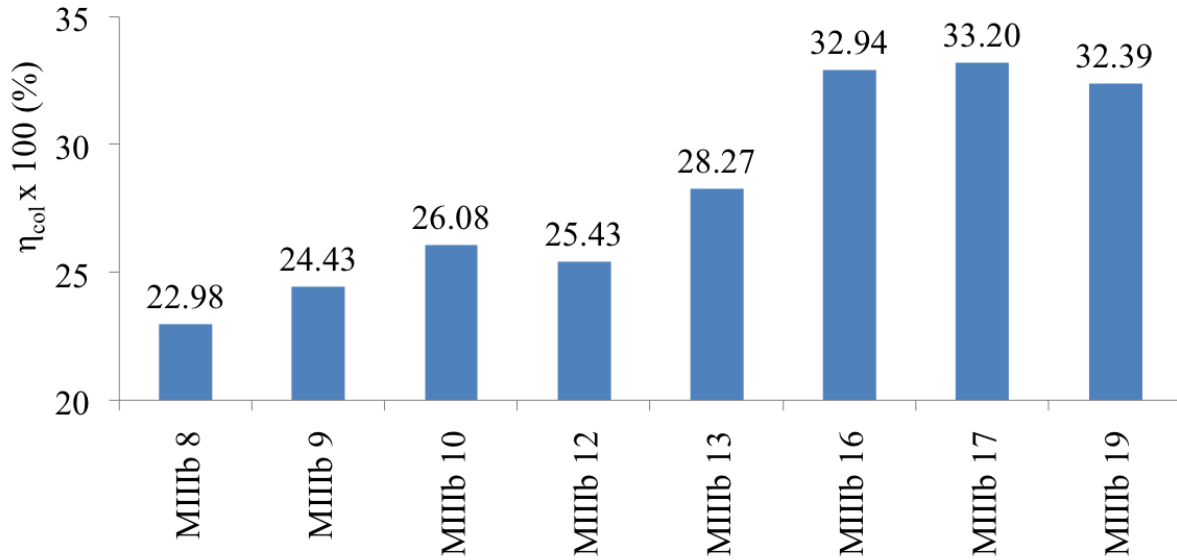

264
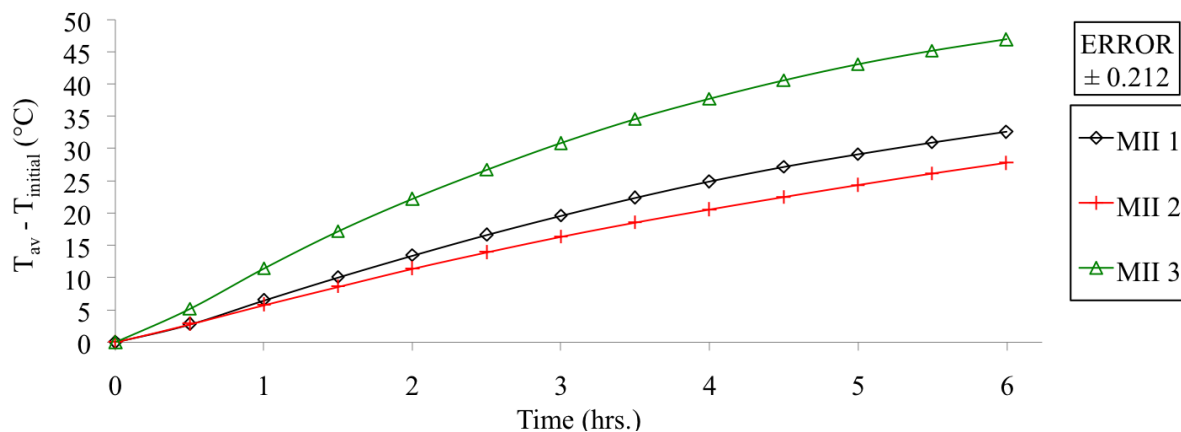
Figure 8: Normalised average store temperatures for MII test 1 to 3 over a 6 hour collection period under
thermally simulated test conditions

269   Mark IIIb (variants IIIa represented similar designs tested to determine heat loss only and did not use the solar
270   simulated flux experimental procedures) was similar to Mark II except with a thermal break and combined inlet
271   and outlet port, designed to reduce heat loss by direct metal to metal conduction from the inner thermal store to

272   the outer vessel lid surface. The design also included a 'Top Hat' disc that isolated vapour from condensing on

273   the upper external surface lid.

274   Selected test collection efficiencies, normalised average store temperatures, store thermocline development and

275   annulus temperature and pressures for Mark IIIa are used to demonstrate performance (Figures 9 and 10).

276

277
278

279   Figure 9: Collection efficiencies for Mark IIIb selected tests under thermally simulated test conditions

280

281
282
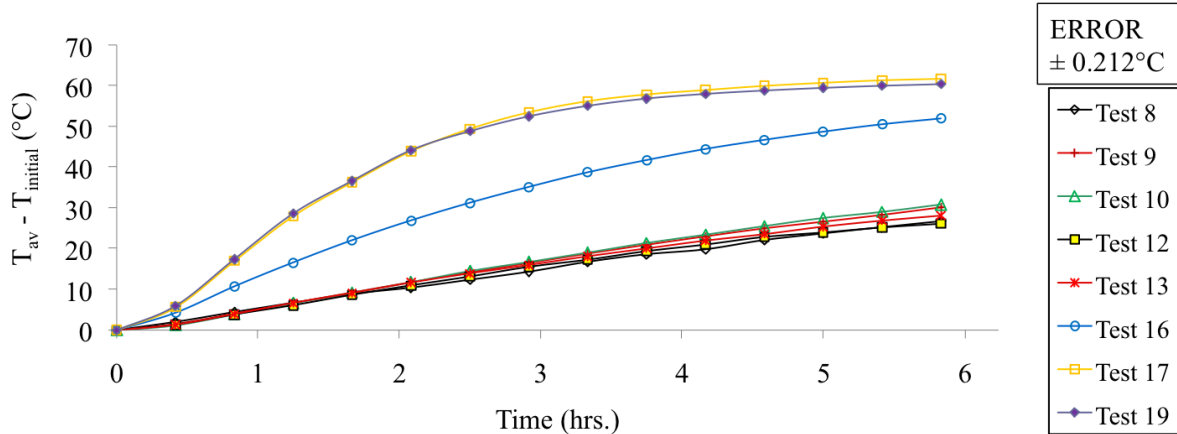
283   Figure 10: Average normalised vessel store temperatures for Mark IIIb selected tests over a 6 hour collection

284   period under thermally simulated test conditions

285

286   Tests MIIIb 17 and 19, which used both capillary matting and a partial vacuum pressure of 150mbar, achieved

287   the highest normalised average temperatures with rapid heat up and maintained higher temperatures. The 6 hour

288   collection efficiencies were 33.2% and 32.39%, respectively as shown in Figure 9 (their 3 hour collection

289   efficiencies were was 41.97% and 40.92%, respectively). Figure 10 shows how the average normalised thermal

290   store temperature for MIIIb 17 and 19 increases more quickly during the first 3 hours than during the remaining

291   collection period indicating that a heat saturation point is reached. This was evidenced in thermocline

292   development where there is rapid stratification during the first three hours after which there is heat saturation in

9

the upper portion of the thermal store. By the 4th hour a steady state position is reached in the upper part of the vessel. At higher pressures, the annulus contains a greater mass of air, which when heated causes greater convective flow and thus better initial transfer from the outer surface to the inner store.

The benefit of the thermal break is shown by the increase in the collection efficiency from 29.82% in MII 3 to 32.94% and 33.2% for tests 16 and 17, respectively. The benefit of the capillary matting is demonstrated by a 29.5% increase in collection efficiency of MIIIb 16 over MIIIb 12 (Top Hat). The effect of the Top Hat on performance can be seen by comparing the annulus sensors and thermoclines. The Top Hat may have the effect of pushing the heat further down the annulus.

Evidence that water within the raised pockets is evaporating and then refilling with condensate is shown by the PT100 4 temperatures, circled in Figure 11. PT100 4 is positioned so as to measure the temperature of liquid PCM 5 mm from the top of the raised pocket. When enough PCM evaporates without the pocket being refilled the sensor will measure the space temperature (just above the pocket liquid level) in the annulus which will be at a higher temperature than the condensate. But when the pocket refills again with condensate the temperature measured will fall back again.
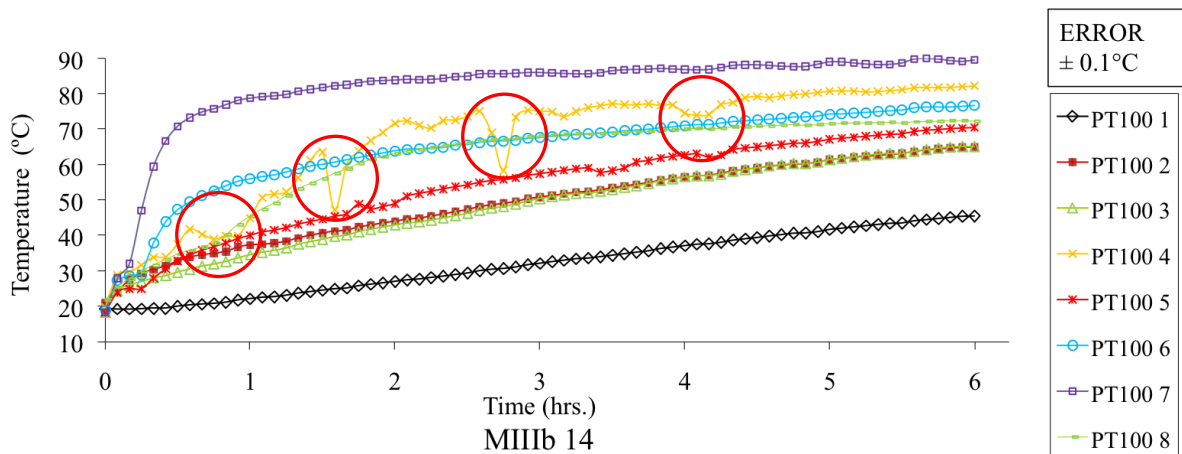

Figure 11: Annulus temperatures every for MIIIb 14 over a 6 hour collection period under thermally simulated test conditions

Mark IV was designed to increase collection efficiency by increasing the amount of PCM in the annulus that was in direct contact with the heat absorbing surface through making the raised pockets longer and thinner. Additionally, the cowl was modified to permit upward flow of vapour but prevent downward flow of condensate (beyond the designated pocket). The results of these design modifications for collection and cool down under thermally simulated test conditions are presented. Selected tests from the test programme are shown to reduce duplication and allow specific design characterisation and performance to be demonstrated more clearly.
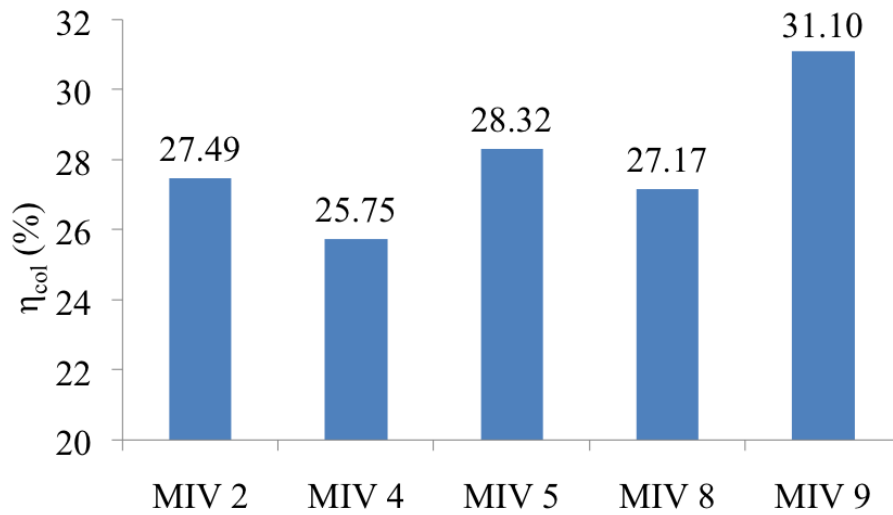
Figure 12: The 6 hour collection efficiencies for Mark IV selected tests under thermally simulated test conditions

The highest collection efficiency as shown in Figure 12 was MIV 9 at 31.1% which was 6% lower than the highest 6 hour collection demonstrated by MIIIb 17. The annulus temperature measurements indicate the presence of a strengthening convective cell in the upper region which reduces the temperature differences in the region as temperature increases. In MIV 5, holes in the cowls allowed a convective cell to be established across more than one region, this reduced temperatures in the upper region whilst increasing the temperature in the middle region. Comparing thermoclines (Figure 13), MIV 9 exhibits a large temperature stratification difference from previous tests, especially after 2 hours, where MIIIb 19 maintained stratification throughout the thermal store indicating strong heat transfer to the top of the thermal store. MIV 9 however has no stratification after three hours in the top 80% of the thermal store suggesting uniform heating of this region. This is supported by analysis inner PT100 sensors situated 500mm from the top of the annulus (half way down) having the same temperature as PT100 sensors at the top of the annulus.
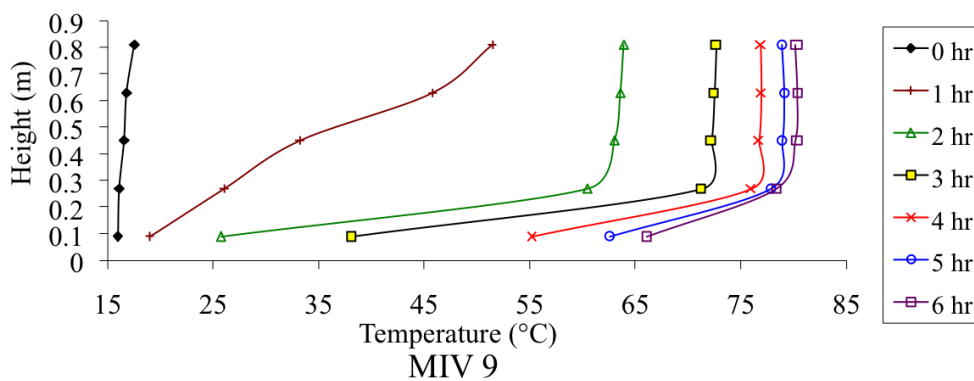

Figure 13: Hourly thermoclines during the collection period of Mark IV 9 under thermally simulated test conditions, (error ± 0.15°C)

344   The lowest system 'U' value (Figure 14) for Mark IV (MIV 1) was 1.27 W $m^{-2}K^{-1}$ at 50mbar 7.6% higher than MI

345   4. The corresponding retention efficiency for MIV 1 was 56.9%. At 150mbar (MIV 3) the system 'U' value

346   increased 15.2% to 1.46 W $m^{-2}K^{-1}$, 8.1% more than the system 'U' value of MI 3 at 100mbar. The reason why

347   Mark IV tests have higher heat losses than Mark I is due to higher average thermal store temperatures. The

348   annulus of MIV units will therefore be warmer and therefore contain more water vapour by mass which will

349   speed up heat loss by convection and conduction. Higher temperatures will also lead to increased radiative heat

350   loss. Comparing tests MIV 1 and 8, the use of capillary matting did not affect the system 'U' value significantly.

351
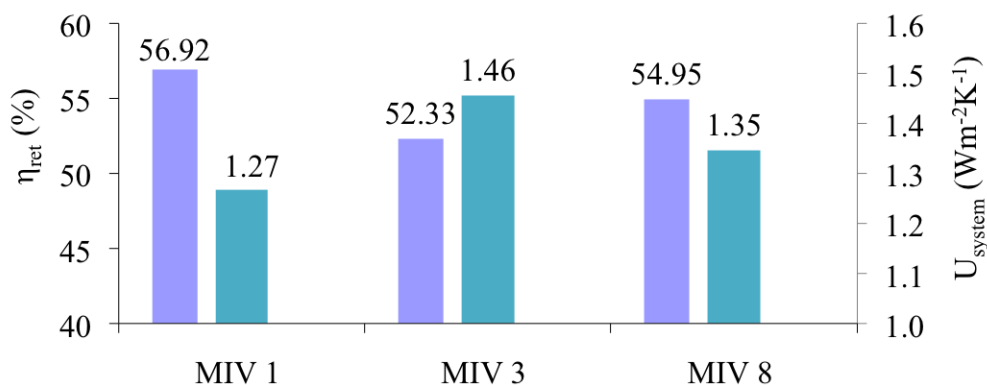
354   Figure 14: Heat transfer coefficient and retention efficiencies for Mark IV tests under thermally simulated test

355   conditions

356

357   Table 2: Summary of prototype performances using various parameters

Mark	Test conditions	Test type	Best 6 hour collection efficiency (%)	Best 6 hour temp rise (°C)	Highest temp achieved (°C)	Best system 'U' value (Wm⁻²K⁻¹)	Best retention efficiency (%)
I	Thermal simulation	Collection/ cooldown	25.39 (MI 4)	23.9°C (MI 4)	42.6°C (MI 1)	1.18 (MI 4)	52.98 (MI 4)
I	Indoor Ambient	Thermal retention				1.07 (MI 6)	46.38 (MI 6)
II	Thermal simulation	Collection/ cooldown	29.82 (MII 3)	47°C (MII 3)	65.7°C (MII 3)	1.75 (MII 3)	39.24 (MII 3)
IIIa	Thermal simulation	Collection	21.63 (MIIIa 11)	19°C (MIIIa 17)	34°C (MIIIa 16)		
IIIa	Indoor Ambient	Thermal retention				0.86 (MIIIa 2)	54.18 (MIIIa 2)
IIIb	Thermal simulation	Collection	33.20 (MIIIb 17)	62°C (MIIIb 17)	78°C (MIIIb 17)		
IV	Thermal simulation	Collection/ cooldown	31.10 (MIV 9)	60°C (MIV 9)	77°C (MIV 9)	1.27 (MIV 1)	56.92 (MIV 1)
IV	Solar simulation	Collection/ cooldown	36.17 (MIV 12)	15.7°C (MIV 12)	35°C (MIV 12)	0.98 (MIV 12)	60.65 (MIV 1)

358
359

360   The optimal performance of each prototype (and selected tests) in terms of collection and retention efficiency,

361   highest temperature achieved and lowest system "U" value is summarised in Table 2. The highest collection

362   efficiency was 36.17% by MIV under simulation conditions. The lowest system 'U' value when PCM was in the

363   annulus was 0.86 W $m^{-2}K^{-1}$ by MIIIa (heat loss only test and not described in this study)) and 0.98 W $m^{-2}K^{-1}$

364   (MIV 12) under thermally simulated conditions when the unit annulus pressure was 50mbar in both cases. The

365   highest average temperature was 78°C achieved by MIIIb 17. The work presented in this study represents

366   progenitor material that has led to significant new work based on the thermal diode principle. Pugsley et al [17]

367   presents a more detailed theoretical analysis of the thermal diode in a Hybrid PVT collector.

368

369   **1.7 Conclusions**

370   A novel thermal diode pre-heat solar water heating system has been designed and developed to be a sustainable,

371   alternative to pre-heat solar water heating systems traditionally used in DHW installations. The concept was

372   based on the operating principles of evacuation and PCMs to offer a cost effective alternative for retro-fit and

373   social housing applications. A number of prototypes were designed, fabricated, tested and evaluated using a

374   bespoke thermal simulation heat flux test facility. The highest 6 hour collection efficiency was 33.2% and the

375   highest 3 hour collection efficiency was 41.97% under thermally simulated conditions for MIIIb 17. The lowest

376   system 'U' value was 0.98 W $m^{-2}K^{-1}$ (MIV 12) under thermal flux testing and no draw-off conditions (or 0.86 W

377    $m^{-2}K^{-1}$ (MIV 12) under heat loss only testing). When the current prototype ICS units are compared with other

378   conventional ICS systems, particularly in terms of thermal retention during non-collection periods, an improved

379   performance is clearly demonstrated [18]. The measured thermal losses were approximately 50% less than other

380   similarly measured systems.

381

382   The study concludes that the system performance is optimal with between 3 to 5 litres of PCM in the annulus at a

383   low partial vacuum pressure (enough to wet the heated surface areas but not so as to contribute significantly to

384   the thermal mass). Other significant enhancements that were shown to improve performance were a high surface

385   area to PCM mass ratio through the use of raised pockets, elongated pockets and capillary matting, use of a

386   transparent cover and heat loss reduction methods such as a vessel thermal break feature for the inlet and outlet

387   ports. Thermal retention was improved through lower partial vacuum pressures and by using the thermal

388   break/combined inlet and outlet and pipe connections made from the vessel base, using stainless steel vessels, a

389   transparent cover and from an increased thermal mass. Thermal store stratification improved through vertical

390   orientation, the use of the Top Hat feature, raised pockets and annulus compartmentalisation, use of a stainless

391   steel inner vessel, thermal break, back insulation and addition of a transparent cover. A system designed upon

392   features exhibited in variants MIIIb 17 and MIV 12 has been shown to be the optimal configuration.

393

394   Through experimental and parametric evaluation, a unique pre-heat ICS solar water heating system has been

395   designed, developed, analysed and presented. Significant steps have been made towards a potential commercial

396   future, but in order to fully realise this goal, much more study is required.

397

400

401   **NOMENCLATURE**

402   A_{unit} surface area of unit (m^2)

403   c_p specific heat capacity of water (J/kgK)

404   m mass of water (kg)

405	$\textbf{mc}_{\textbf{system}}$	thermal capacity (J/K)
406	$\textbf{Q}_{\textbf{col}}$	thermal energy collected (J)
407	$\textbf{Q}_{\textbf{supplied}}$	thermal energy supplied (J)
408	$\textbf{T}$	temperature (°C/K)
409	$\textbf{U}_{\textbf{system}}$	system heat loss coefficient (W m^{-2}K^{-1})
410	$\boldsymbol{\Delta t}$	time (secs)
411	η	efficiency
412	σ	stratification index
413	$\varnothing$	diameter

414

Subscripts (415)

416

417	**amb**	average ambient temperature
418	**amb**	average ambient temperature
419	**av**	average water temperature
420	**av,b**	average water temperature at bottom 1/5 of vessel
421	**av,t**	average water temperature at top 1/5 of vessel
422	**end**	average water temperature at end of heating period
423	**final**	average final water temperature at end of cooling period
424	**initial**	average initial water temperature
425	**initial,c**	average initial water temperature at start of cooling period
426	**ret**	heat loss retention
427	**start**	average water temperature at start of heating period

428

REFERENCES

430 [1] Smyth M, Eames PC and Norton B, 2006. Integrated Collector Storage Solar Water Heaters. Renewable and

431 Sustainable Energy Review, Vol. 10, Iss.6, pp 503-538

432 [2] Tripanagnostopoulos Y & Yianoulis P, 1992. Integrated collector/storage systems with suppressed thermal

433 losses. Solar Energy, Vol. 48, No. 1, pp 31 - 43

434 [3] Baer S, 1975. Breadbox Water Heater Plans. Zomeworks Corporation, P.O. Box 25805, N.M. 87125, U.S.A.

435 [4] Bishop RC, 1983. Superinsulated Batch Heaters for Freezing Climates. Proc. of the 8th National Passive

436 Solar Conference, Sante Fe, New Mexico, U.S.A., Sept. 7-9, pp 807-810

437 [5] Schmidt C, Goetzberger A & Schmid J, 1988. Test Results and Evaluation of Integrated Collector Storage

438 Systems with Transparent Insulation. Solar Energy, Vol. 41, No. 5, pp 487-494

439 [6] Schmidt C & Goetzberger A, 1990. Single-Tube Integrated Collector Storage Systems with Transparent

440 Insulation and Involute Reflector. Solar Energy, Vol. 45, No. 2, pp 93-100

441 [7] Stickney BL & Nagy C, 1980. Performance Comparisons of Several Passive Solar Water Heaters. Proc. of

442 the 5th National Passive Solar Conference, Amherst, Massachusetts, U.S.A., pp 1071-1075, Oct. 16-26

443 [8] Burton JW & Zweig PR, 1981. Side by Side Comparison Study of Integral Passive Solar Water Heaters.

444 Proceedings of the 6th National Passive Solar Conference, Portland, Oregon, U.S.A., Sept. 8-12, pp 136-140

445   [9] Bainbridge DA, 1981. The Integral Passive Solar Water Heater Book. The Passive Solar Institute, PO Box
446   722, Davis, CA 95616, U.S.A

447   [10] Tripanagnostopoulos Y & Souliotis MK, 2003. Double tank ICS solar systems. ISES Solar World Congress,
448   Goteborg, Sweden

449   [11] De Beijer, H.A. "Product Development in Solar Water Heating", Proc. of the 5th World Renewable Energy
450   Congress, Florence, Italy, pp 201-204, September 1998

451   [12] Anon. 2007a. Solar Heating – Domestic Water Heating Systems- Part 5: System Performance
452   characterization by means of whole-system tests and computer simulation. BS ISO 9459-5:2007, British
453   Standards Institution, London, UK

454   [13] Anon. 2007b. Chartered Institute of Building Services Engineers Environmental Guide A. 7th Edition,
455   Merton, UK

456   [14] Gnafakis C & Manno VP, 1989. Transient destratification in a rectangular enclosure. Transactions of the
457   American Society of Mechanical Engineers, Vol. 111, pp 92 -99

458   [15] Visser H & Van Dijk HAL, 1991. Test procedures for short term thermal stores. Kluwer Academic
459   Publishers, Dordrecht, The Netherlands

460   [16] Quinlan P, 2010. The Development of a Novel Integrated Collector Storage Solar Water Heater (ICSSWH)
461   Using Phase Change Materials and Partial Evacuation. PhD Thesis, University of Ulster

462   [17] Pugsley A, Smyth M, Mondol JB, Zacharopoulos A & Mattia L, 2016. Experimental characterisation of a
463   flat panel integrated-collector-storage solar water heater featuring a photovoltaic absorber and a planar liquid-
464   vapour thermal diode. 11th ISES EuroSun Conference, October 2016, Majorca, Spain

465   [18] Singh R, Lazarus IJ & Souliotis M, 2016. Recent developments in integrated collector storage (ICS) solar
466   water heaters: A review. Renewable and Sustainable Energy Reviews. Vol. 54, pp 270-298

467